

1 **Investigating the impact of copper leaching on combustion**
2 **characteristics and particulate emissions in HPCR diesel engines.**

3

4 A. La Rocca, A. Ferrante, E. Haffner-Staton, A. Cairns Powertrain Research Group, The University
5 of Nottingham

6 A. Weilhard, V. Sans Chemical Engineering, The University of Nottingham

7 A.P. Carlucci, D. Laforgia – Research Centre for Energy and Environment, University of Salento

8

9 Key words: Copper, Soot, Fuel additives, Combustion, Catalyst

10 **Abstract**

11

12 A helicoidally shaped copper duct was installed along the fuel line just before the high
13 pressure pump. The impact of fuel contamination from this copper duct on combustion
14 and emission characteristics of a Direct Injection High Pressure Common Rail (DI HPCR)
15 diesel engine was investigated. The copper duct constitutes the core of a fuel conditioning
16 device, powered from the battery. A single cylinder Ricardo Hydra research engine with
17 the cylinder head, piston assembly and crankshaft from a production 2.2 L DI diesel engine
18 was used in the investigation. Combustion characteristics were analysed via post-
19 processing pressure measurements, while an AVL Smoke Meter was used to monitor
20 particulate emissions. A diesel fuel with a copper content of less than 0.2ppm was used.
21 Inductively coupled plasma mass spectrometry (ICP-MS) analysis of the fuel showed
22 copper leaching into the fuel, with 1 ppm Cu being found in the fuel after flowing through
23 the helicoidally shaped duct. Recirculation of fuel to the tank led to an increase of Cu
24 concentration in the fuel. A pilot plus main strategy was used to achieve a target Brake
25 Mean Effect Pressure (BMEP) typical of medium load. Soot reduction in the range of 7-
26 14% was measured when the device was connected to the fuel line, compared to the
27 baseline. The initiation and early development of combustion was also investigated using

28 an unstirred, quiescent combustion chamber with optical access, and the results
29 corroborate findings from the engine work.

30 **Introduction**

31

32 Recent predictions of the demise of the automotive internal combustion engine (ICE) have
33 been greatly exaggerated, as hybrids are a key part of the long-term transport plan. Mild
34 hybrids with clean ICEs are forecast to be popular in small and medium sized cars, while
35 heavier commuter and heavy-duty long haul vehicles will still be reliant on diesel. The
36 recent Bosch breakthrough offers an opportunity for aggressive emission reductions (i.e.
37 5 times below the legal limit). Regulations will continue to restrict further the exhaust
38 emissions, with particular attention paid to new pollutants and particulate emissions. It is
39 likely that particulates will be limited using new number and size-based metrics with
40 thresholds as low as 10nm or less. Greater emphasis will also be given to pollutant
41 emissions studies based on real-driving conditions, in contrast to defined test procedures.
42 Though particulate filters are effective when employed to trap particulate matter in the
43 exhaust gas stream, their use comes at the cost of increased backpressure and consequent
44 decrease in engine efficiency and fuel economy. Additional decreases in fuel economy arise
45 due to filter regeneration events [1]. Moreover, while engine calibration over the
46 Worldwide harmonized Light vehicles Test Cycle (WLTC) allows for the limits to be met,
47 real driving emission, cold start and performance subsistence over the entire vehicle life
48 constitute a real challenge. These challenges have recently been faced also by the modern
49 gasoline direct injection engines [2,3]. Researchers' efforts have been focusing on
50 reducing formation of particulate matter via improving combustion chamber design, fuel
51 injection strategies, combustion modes, and new fuels. Considerable numbers of diesel
52 vehicles, including registered agricultural, construction vehicles and other off-
53 road applications such as boats, currently in use are well behind with regards to Euro
54 standards compliance. Retrofitting of particulate filters is challenging due to high soot
55 emission levels causing premature failure of these after-treatment devices [4]. To meet
56 the stringent emissions legislation governing air pollutants released into the atmosphere

57 requires the addition of new technology to older systems aiming at needs to either prevent
58 or reduce the formation of particulate matter to levels that are manageable for the
59 filtration systems.

60 Fuel nanoparticles added to the diesel fuel can have positive effect on engine behaviour;
61 in particular, an interesting route to achieve lower particulate emission is the use of
62 metallic additives. The presence of particles in the fuel can also be due to the interaction
63 between fuel and Fuel Injection Equipment (FIE). Fuel contamination with particles greater
64 than $4\mu\text{m}$ can have important consequences on FIE lifetime [5]. The catalytic activity of
65 metallic-based fuel additives has been investigated widely [6,7]. In their comprehensive
66 review of the effect of metal nanoparticles on combustion, Saxena et al. [8] provided a
67 pathway to maximise the potential of metal nanoparticles in fuels. Keskin et al. [9] found
68 that fuel properties such as pour point, cloud point, and viscosity change with addition of
69 metallic based additives. Typically, mechanical mixing of nanoparticle or the so called sol-
70 gel method are used to prepare the nanometal mixture [10,11], although the cost of
71 nanopowder can be expensive. Suspensions of sonicated metal nanoparticles require
72 addition of surfactants to achieve stable and homogeneous mixtures [11]. Soluble
73 additives such as ferrocene and iron pentacarbonyl can also be used [12-14]. In the study
74 proposed by Keskin et al. [15,18] the addition of $8-16\ \mu\text{Mol L}^{-1}$ of metal-based additive
75 resulted in a decrease in fuel consumption up to 4%, and smoke opacity up to 30%. The
76 addition of Fe_3O_4 nanoparticles in very low concentration is reported to have a considerable
77 effect on diesel engine characteristics [14]. Addition of copper oxide to diesel fuel using
78 the sol-gel method is reported to lead to a marginal increase in performance, but a rather
79 significant decrease in pollutants emitted by a single cylinder diesel engine. Work by Lenin
80 et al. found that manganese showed an even stronger influence on emission reduction [9].
81 The metallic additive is seen to enhance the combustion process and shorten the ignition
82 delay. A reduction of 7% in specific fuel consumption was also revealed when using fuels
83 with sonicated metal nanoparticles (Al, Fe, B) [10]. A flame sustained over a longer period
84 was noticed. In 2016, Gumus et al. [16] reported that the use of copper nanoparticles in
85 diesel increases the ignition probability and has a positive effect on reducing brake specific

86 fuel consumption and noxious emissions. Similarly, Tyagi et al. observed enhanced ignition
87 probability of the diesel fuel with the addition of nanoparticles [17]. They suggested further
88 investigation on the effect of copper and aluminium nanoparticle size as the metal
89 nanoparticles are surface reactive and surface area can be of importance. The mechanisms
90 governing the working principle and the development of a suitable theoretical model are
91 still debated. Metallic catalyst reacts firstly with water producing hydroxyl radicals and
92 enhancing soot oxidation; then, with carbon atoms in the soot lowering the oxidation
93 temperature [18]. Additives are generally nanosized as more stable than microscale
94 suspensions and require a lower activation energy [19]. The effect of addition of iron,
95 cerium or copper, in combination with the Diesel Particulate Filter (DPF) has been studied
96 in [20-21]. The analysis has demonstrated that the presence of DPF determines: always
97 an increase of benzene and 1,3-butadiene (both carcinogenic); always a reduction of
98 carcinogenic PAH; an increase of PCDD/F if the fuel is added with copper (usually between
99 10 and 50 $\mu\text{g/g}$) but only in presence of significant amounts of chlorine.

100 Several works in the literature have also analysed the effect of fuel on copper corrosion
101 [22-27]. Corrosion behaviour of aluminium, copper and stainless steel in diesel was
102 investigated by Fazal et al. [26] showing that the exposed metal surfaces are indeed
103 susceptible to corrosion. Biodiesel was found to be more corrosive than diesel, with copper
104 being the least resistant forming comparatively more corrosion products than other metals
105 [23-25]. A corrosion rate of $23\mu\text{m/year}$ was reported for copper exposed to biodiesel [23].
106 Albeit the effect of copper leaching on fuel properties has been quantified [24-26], its
107 impact on emissions and combustion characteristic has not.

108 In this work, a new fuel conditioner device (from here on referred to as "device"),
109 constituted by an helicoidal copper duct surrounded by electromagnetic coils and installed
110 just before the high pressure pump, was tested and its effect assessed on the combustion
111 characteristics and particulate emissions of a modern DI HPCR diesel engine. Several
112 devices, the majority of which are based on the application of a magnetic field along the
113 fuel supply line, have been proposed in the past to improve fuel economy and reduce
114 emissions. Some of these devices underwent through a thorough assessment carried out

115 by the Environmental Protection Agency (EPA) [28,29]. At the end of the experimental
116 campaign, conducted during the '80, it was demonstrated that, with either road or
117 dynamometer testing, such devices failed to improve vehicle fuel economy or reduce
118 emissions. However, it must be emphasized here that the tested devices were designed
119 to be installed on (pre-eighties) gasoline engines with the goal to reduce carbon monoxide,
120 unburned hydrocarbons and nitrogen oxides emission levels; given the inherent low soot
121 emission propensity of these engines, Particulate Matter (PM) measurements were
122 therefore not carried out.

123 The engine testing reported in this work suggests that, when the device is used, leaching
124 of metals in the fuel takes place; these fuel borne catalysts have then a role in enhancing
125 soot oxidation lowering particulate emissions. Leaching of additives into the fuel is
126 potentially an interesting addition mechanism which could allow for ions, or subnanometric
127 particles, to be released at the point of need.

128

129

130 **EXPERIMENTAL SETUP**

131

132 **Single cylinder DI diesel engine**

133

134 The investigation has been carried out on a single cylinder Ricardo Hydra, with the cylinder
135 head, piston assembly and crankshaft from a production 2.2 L DI diesel engine. The swept
136 volume was stated as 550 cc, bore 86 mm, and stroke 94.6 mm (four valves per cylinder;
137 2 intake and 2 exhaust). The compression ratio (CR) was measured as 15:1. Diesel was
138 supplied to the HPCR fuel injection system by a Bosch high pressure pump rated to
139 2000 bar. The 8-hole piezo-electric injector was centrally mounted. The engine was kept
140 at test temperature by circulating "coolant" through the block and head. Heaters were
141 used to directly increase the coolant and oil temperature. A 3 kW immersion heater from
142 Watlow Industries was used to regulate the coolant fluid, and two Eltron Chromalox sump
143 mounted heaters were used for the oil. The additional heat input from these heaters was

144 necessary since the single cylinder engine does not produce sufficient heat to achieve
145 typical warm operating conditions. A Carter M3 series cooling tower was used rather than
146 a radiator for heat rejection. An 80 L plenum placed before the intake was used to provide
147 a reservoir of constant temperature and pressure intake air. A reference fuel with Cetane
148 Index 54.7 was used throughout these tests. Pressure transducers and thermocouples
149 were used to monitor operation.

150 Cylinder pressure was measured using a Kistler 6125B quartz pressure sensor rated to
151 250 bar peak pressure. An optical shaft encoder with half degree crank angle resolution
152 output (1440 pulses per engine cycle) was used as trigger for LabVIEW data acquisition
153 system, through which many system variables are measured and stored every half crank
154 angle step. The encoder top dead centre (TDC) marker was set to coincide with piston TDC
155 in the cylinder. To ensure accurate TDC position, an AVL 402 dynamic probe was used.
156 Accurate measurement was required since small errors in TDC measurement can result in
157 large calculation errors in IMEP. The shaft encoder was set to within 0.5 °CA compared to
158 TDC measured using the capacitance probe. Other measurements such as air, coolant,
159 exhaust, fuel, and oil temperatures were recorded on the time based National Instruments
160 Data Acquisition hardware and Labview software. A dedicated software was used to
161 communicate with the engine's ECU. The software provided control of various injection
162 parameters such as injection quantity, number of injections, injection timing (and
163 therefore separation) and rail pressure. Up to six injections per cycle were possible on this
164 system but two were the maximum used in this study (one pilot injection followed by a
165 main injection).

166 The test conditions chosen reflect low-speed, medium load conditions. The engine was run
167 initially at the desired test speed, by which time both engine speed and fuel rail pressure
168 had stabilised to their respective set point values. The fuel injection was then enabled, and
169 injection quantities and timings were held constant. The dynamometer was used to
170 maintain the set point engine speed throughout the test. The use of a single cylinder
171 research facility with dynamometer control allows detailed analysis of combustion events
172 by eliminating variables such as engine speed and cylinder to cylinder

173 variations/interactions, a technique previously applied by McGhee et al. [30,31] and
174 MacMillan et al. [32]. Complete control over injection parameters was possible throughout
175 the investigation. An AVL Smoke Meter was used to measure the soot concentration (in
176 mg/m^3) emitted by the DI diesel engine used in the present investigation. The variable
177 sampling volume and the thermal exhaust conditioning ensure an extremely high
178 reproducibility. The instrument can be used not only on large engines but also on light
179 duty engines independent of their generation. The instrument has a high measurement
180 resolution ($10\mu\text{g}/\text{m}^3$) and low detection limit ($20\mu\text{g}/\text{m}^3$).

181

182 The conditioning device was installed in the fuel line just before the high pressure pump.
183 Two sets of test conditions were investigated: with device powered (WDP conditions) and
184 with device not powered (WDNP conditions).

185

186

187 **Quiescent combustion chamber**

188

189 The initiation and early development of combustion that occurs before the effect on
190 cylinder pressure is measureable is of interest here for the two sets of test conditions:
191 WDP and WDNP. The study of combustion initiation by glow plug was carried out using an
192 unstirred, quiescent Constant-Volume Combustion Chamber (CVCC). This has optical
193 access through a quartz window giving a view normal to the plate in which the injector
194 and glow plug were mounted. The spacing between the injector and glow plug was the
195 same as in the single cylinder engine.

196 The internal volume of the CVCC is roughly cylindrical with a height of 190mm and a
197 bore of 100mm. The experimental facility is shown schematically in Figure 1. The same
198 design of HPCR fuel injection system and fuel injector were used as employed on the
199 engine. The injector was piezo-electric with 8 nozzle holes, the same design as used in the
200 single cylinder engine. The holes have a diameter of $120\mu\text{m}$. The volume of the CVCC is
201 large compared to the clearance volume of the engine cylinder, being CVCC used here only

202 to examine the initial development of combustion which takes place at constant pressure.
203 The rationale is to investigate whether the device has an impact on initiation and early
204 development of combustion. Prior to fuel injection, air in the CVCC is quiescent. Whilst this
205 would not usually reproduce in-cylinder conditions, at the low engine speeds, associated
206 with idling, turbulence levels are low, and motion in the vicinity of the glow plug just prior
207 to the start of combustion is dictated by the momentum of the fuel sprays, entrainment,
208 and mixing.

209 Pressure inside CVCC and internal tip temperature of glow plug and injection
210 parameters such as injection separation, timing, and number of injections were controlled
211 and recorded using National Instruments USB-6351 X Series Data Acquisition hardware
212 and Labview software. Rail pressure was monitored by a pressure sensor on the fuel rail.
213 A pressure control valve was utilized to adjust pressure in the high pressure fuel pump by
214 means of PID control.

215
216

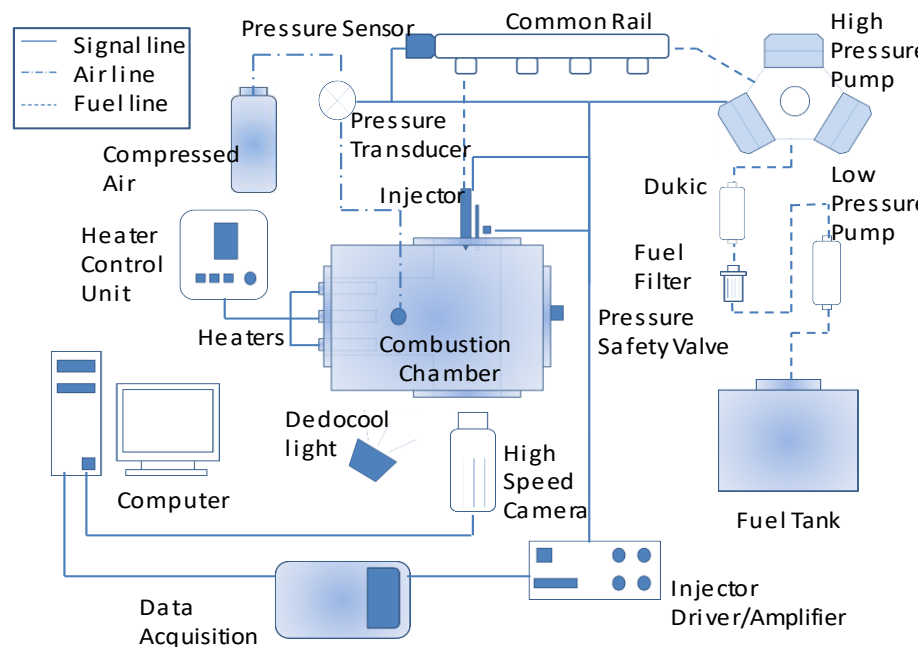


Figure 1 - Schematic representation of the CVCC test rig architecture

221 High-speed video recordings were made of the fuel sprays penetrating the chamber and,
222 if initiation was successful, of the first appearance and growth of luminous emissions in
223 one or both sprays adjacent to the glow plug. The camera used was a Phantom V12.1
224 CMOS high-speed camera capable of 6,242 frames per second at a maximum resolution
225 of 1280x800 pixels. The settings of focal length, aperture and exposure time were
226 respectively 105mm, f/3.5 and 100 μ s. One Dedocool tungsten light was used to illuminate
227 the fuel sprays. A fixed fuel injection strategy of single pilot and main was used throughout
228 the set of experiments. The first luminous emissions have been taken to indicate the start
229 and sites of combustion, as suggested in [33]. The subsequent growth of the luminous
230 area has been taken to indicate successful ignition.

231

232

233 **Inductively coupled plasma mass spectrometry (ICP-MS)**

234

235 Copper detection was carried out using ICP-OES (Inductively coupled plasma - optical
236 emission spectrometry) PerkinElmer Optima 3300 DV with autosampler AS90 Plus and
237 controlled with Perkin Elmer Winlab software. ICP operational conditions occurred with
238 Cross-flow GemTip nebuliser, Ryton Scott type spray chamber; details are in Table 1.

239

240 *Table 1 - Operational conditions of ICP-OES*

Plasma flow	15 L/min
Aux flow	0.5 L/min
Neb flow	0.8 L/min
RF Power	1300W
Pump	1.0 ml/min
Wavelength measured	Cu 324.752, Cu 327.393

241

242

243 Calibration standards were prepared from single element standard solutions (Romil
244 PrimAg) diluted with 4% HNO₃ prepared from 68% nitric acid (Fisher PrimarPlus). All
245 solutions were prepared using Milli-Q ultrapure water (18.2 M Ω cm⁻¹).

246 In order to trace metals in the samples, ICP technique has been used. The composition of
247 metals in water diluted samples is determined using plasma and spectrometer; the sample
248 is conducted by a peristaltic pump through a nebulizer into a spray chamber that produced
249 aerosol; the latter is lead into an argon plasma which is generated at the end of a quartz
250 torch by a cooled induction coil, through which a high frequency alternate current flows.
251 Consequently an alternate magnetic field is induced which accelerated electrons into a
252 circular trajectory and, due to collision between the argon atoms and the electrons,
253 ionization occurs, giving rise to a stable plasma (6000-7000 K). Due to the thermic energy
254 taken up by the electrons, they reach a higher "excited" state. When the electrons drop
255 back to ground level, energy is liberated as photons. Each element has an own
256 characteristic emission spectrum that is measured with a spectrometer, so the light
257 intensity on the wavelength is measured and, with the calibration, converted into a
258 concentration.

259

260

261 **Heat release analysis of combustion**

262

263 The rate of release of the fuel's chemical energy through the engine combustion process
264 is commonly referred as heat release rate (HRR). In this work, the calculations mostly
265 follow the approach suggested in Heywood [34]. The experimentally acquired in-cylinder
266 pressure data was used to provide the heat release rate. As described in [34] the in-
267 cylinder pressure changes with crank angle as a result of cylinder volume change,
268 combustion of fuel, heat transfer to the chamber walls, flow into and out of crevice regions,
269 and leakage; where the first two of these effects are the most relevant. Heat release
270 analysis provides an insight of the combustion phenomenon inside the engine cylinder. By
271 analysing cumulative and heat release rate the combustion phasing, the burning rate, and
272 the degree of completeness of combustion can be quantified and compared. Heat release
273 rates were determined from cylinder pressure data using [34]:

274

275

$$\frac{dQ_n}{d\theta} = \frac{\gamma}{\gamma - 1} p \frac{dV}{d\theta} + \frac{1}{\gamma - 1} V \frac{dp}{d\theta}$$

277

278 The four stages typically recognisable in a compression ignition engine are ignition delay,
279 premixed combustion, mixing-controlled combustion and late combustion; each stage can
280 usually be identified on the HRR curve [34]. In this work, the ignition delay is defined as
281 the time between the start of injection (SOI) and the start of combustion (SOC). In this
282 work, SOC has been defined as the point after SOI at which the rate of heat release is
283 equal to $2J/^\circ$. During the ignition delay stage, part of the injected fuel vaporises and mixes
284 with air; as SOC occurs, the premixed combustion stage begins. During the premixed
285 stage, the air/fuel mixture close to stoichiometric proportion that has formed throughout
286 the ignition delay period burns. After this stage, the heat release and burn rate are dictated
287 by fuel vaporisation and mixing rates; this stage of the combustion is known as mixed
288 controlled phase. The last stage is a late combustion phase characterised by low rates of
289 heat release.

290

291

292 **Results and discussion**

293

294 1. Single Cylinder DI Engine Tests

295

296 An initial dataset was collected as baseline for comparison with the device not
297 connected in the fuel line (WO conditions). A pilot injection of 2mg fuel was followed by a
298 main injection of 10mg fuel. The engine was run at a constant engine speed of 1000rpm.
299 Once a steady state was reached, measurements were taken recording torque, brake
300 mean effective pressure (BMEP), and exhaust soot concentration. A summary of the results
301 is given in Table2. Average value (AVG) and Standard Deviation (STD) were calculated

302 over 15 soot measurements, while heat release rate was calculated on average of 200
303 pressure traces acquired.

304

305

306 *Table 2 - Test operating condition and measurements of torque, BMEP and soot with the*
307 *device not connected along the fuel line (WO conditions). Total fuel injected 12mg/str.*
308 *AVG stands for average and STD for standard deviation.*

pilot		main		AVG Torque	AVG BMEP	AVG Soot	STD Soot
°ATDC	mg	°ATDC	mg	Nm	bar	mg/m ³	mg/m ³
-12	2	-4	10	24.7	5.7	2.19	0.22

309

310

311 When the device was powered for the first time (WDP conditions), an increase in torque
312 and BMEP was noticed, together with a 10% decrease in the average soot concentration
313 measured using the AVL smoke meter. A summary of the results is given in Table 3.

314

315

316 *Table 3 - Test operating condition and measurements of torque, BMEP and soot with the*
317 *device connected and powered along the fuel line (WDP conditions). Total fuel injected*
318 *12mg/str. AVG stands for average and STD for standard deviation.*

pilot		main		AVG Torque	AVG BMEP	AVG Soot	STD Soot
°ATDC	mg	°ATDC	mg	Nm	bar	mg/m ³	mg/m ³
-12	2	-4	10	26.3	6.0	1.98	0.18

319

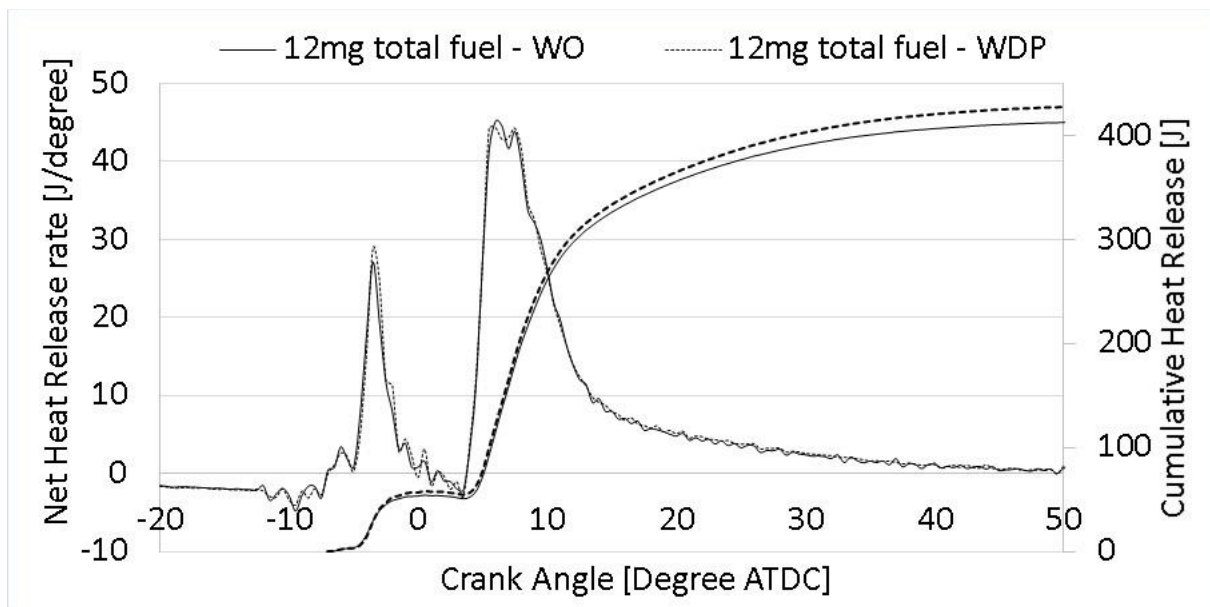
320

321

322 In Figure 2, the heat release rate and the cumulative heat release of the two test conditions
323 from Table 2 and Table 3 are compared. Combustion characteristics and heat release were
324 investigated to understand the reasons behind the measured soot reduction. In all the
325 tests, fuel starts to combust shortly after fuel from main injection enters the combustion

326 chamber, with a measured ignition delay of 5.5CA degrees. For both cases (WDP and WO
327 conditions) the ignition delay was the same. This suggests that physical/chemical delay
328 and fuel/air mixture preparation before ignition is not the reason for the difference in soot
329 concentration measured in the exhaust stream. A greater heat release is observed during
330 the premixed combustion, and overall during the entire combustion process when the
331 device is powered (WDP conditions).

332



333

334

335 *Figure 2 - Comparison of the heat release rate and the cumulative value. WO and WDP.*
336 *Injection strategy pilot plus main 12mg of fuel injected per cycle. Day 1*

337

338 It was then decided to reduce the fuel quantity in the main injection with the aim to match
339 the torque and BMEP given in Table 2. Pilot injection quantity was kept constant at 2mg
340 per stroke while 9.25mg of fuel was injected at 4 degrees before top dead centre (BTDC).
341 As summarised in Table 4, this also resulted in a soot concentrations that were 25% lower
342 than the value reported in Table 2.

343

344

345 *Table 4 - Test matrix and measurements of torque, BMEP and soot with the device*
346 *connected and powered along the fuel line (WDP conditions). Total fuel injected*
347 *11.25mg/str. AVG stands for average and STD for standard deviation.*

pilot		main		AVG Torque	AVG BMEP	AVG Soot	STD Soot
°ATDC	mg	°ATDC	mg	Nm	bar	mg/m ³	mg/m ³
-12	2	-4	9.25	24.4	5.6	1.63	0.095

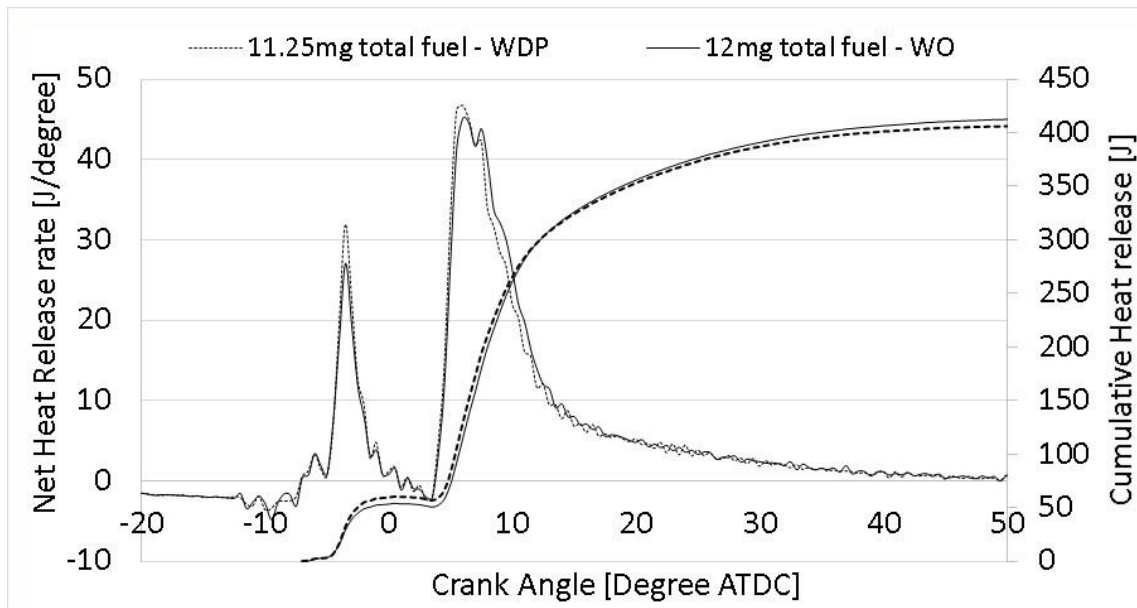
348

349

350 The cumulative heat release, and the rate of heat release for the reduced fuelling with the
351 device in WDP conditions is compared to the 12mg total fuel case in WO conditions. Results
352 are summarised in Figure 3. Despite there being less fuel injected, a higher spike in HRR
353 and cumulative heat release is noticeable in the premixed phase of combustion. Overall,
354 however, the cumulative heat released by combustion is slightly lower for the 11.25mg,
355 WDP conditions.

356

357



358

359

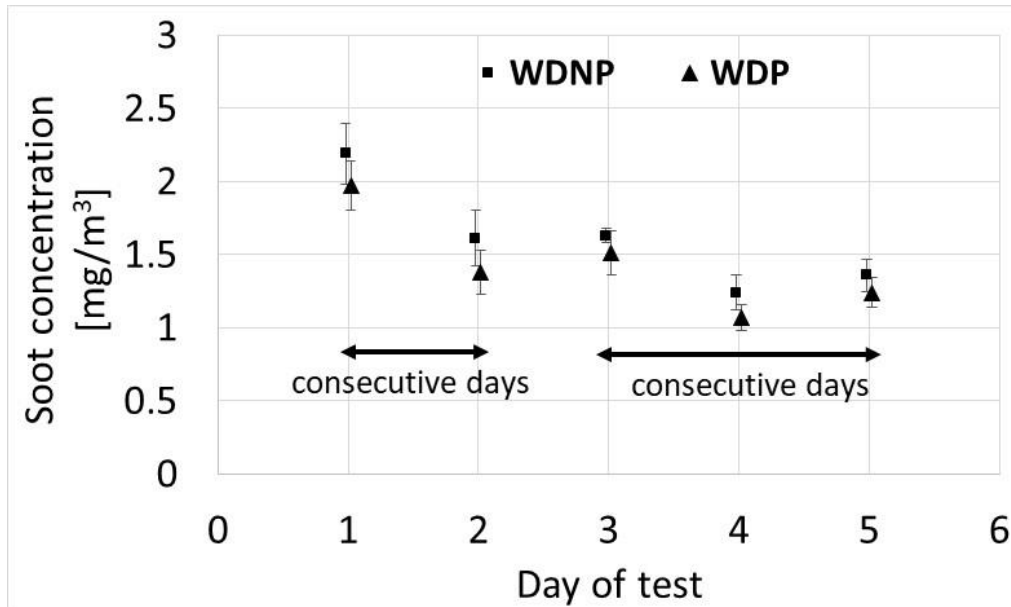
360 *Figure 3 - Comparison of the heat release rate and the cumulative value. 12mg of fuel*
 361 *injected per cycle WO, and 11.25mg of fuel injected per cycle in WDP conditions. Injection*
 362 *strategy: pilot plus main, 12mg of fuel injected per cycle.*

363

364 The findings described above were generally true for all test conditions in day one. Four
 365 more days of engine testing were carried out to corroborate the findings of the first day of
 366 testing. The device was left in the fuel line but electrically disconnected (WDNP conditions).
 367 The fuel tank and fuel line were not flushed, and the fuel filter was not replaced. The fuel
 368 tank was not refilled during the first day of engine testing. Day 2 started with roughly half
 369 a tank of fuel from the previous day, and was refilled towards the middle of the day. On
 370 the subsequent days of engine testing, the fuel tank was regularly refilled throughout the
 371 day. On each day of testing the same test point was repeated several times without
 372 powering the connected device (WDNP conditions), and then again with the device
 373 powered (WDP conditions). Over 200 tests and soot measurements were carried out in
 374 this period.

375 An overall decrease in the amount of soot emitted was noticed over the five days of testing,
 376 as shown in Figure 4. In detail, a gradual decrease in the soot emission was noticed even
 377 when the device was not powered (WDNP conditions) from 2.19mg/m³ (day 1), to 1.61

378 mg/m³ (day 2), and to 1.25 mg/m³ (day 4). Moreover, as shown in Figure 4, each day of
 379 testing when the device is powered a further 8-14% reduction in soot emission was
 380 observed. Details of the results are reported in Table 5.



381
 382 *Figure 4 - Comparison of the average soot concentration collected over five days of testing*
 383 *in WDNP and WDP conditions; over 200 tests and soot measurements were carried out in*
 384 *this period. Injection strategy: pilot plus main injections, 12mg of fuel injected per cycle.*

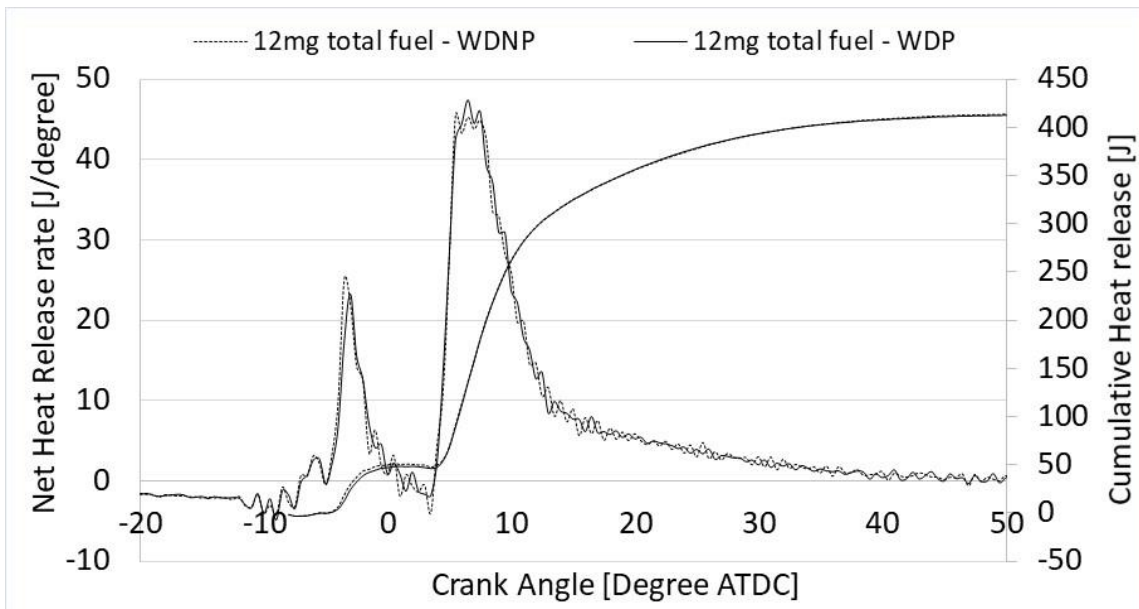
385
 386 *Table 5 - Comparison of soot concentration results collected over five days of testing; over*
 387 *200 tests and soot measurements were carried out in this period. AVG stands for average*
 388 *and STD for standard deviation.*

		With device not powered (WDNP conditions)		With device powered (WDP conditions)	
	Soot reduction [%]	Average Soot conc. [mg/m ³]	STD of Soot conc. [mg/m ³]	Average Soot conc. [mg/m ³]	STD of Soot conc. [mg/m ³]
1st day	9.64	2.19	0.22	1.98	0.18
2nd day	14.04	1.61	0.19	1.39	0.15
3rd day	7.36	1.63	0.05	1.51	0.15
4th day	13.92	1.25	0.12	1.08	0.09
5th day	9.14	1.36	0.11	1.24	0.10

389

390
391
392
393
394
395
396
397
398
399

On each day of engine testing, a reduction of soot emissions is significant and measurable. After the first day of testing the gains on work output and heat release between powering (WDP condition) and not powering (WDNP condition) the device cases become less apparent. BMEP varied in the range 5.6-5.9 bar and a clear trend was not identified. Comparison of cumulative and rate of heat release are given in Figure 5, suggesting that the catalyst in the fuel promotes soot oxidation rather than affecting chemical or physical ignition delay.



400
401
402
403
404
405
406
407
408
409

Figure 5 - Comparison of cumulative heat release and heat release rate. Test 61 run in WDNP conditions and test 92 in WDP conditions. Injection strategy: pilot plus main injections, 12mg of fuel injected per cycle.

A higher BMEP target of 7.6bar was also investigated. The amount of fuel injected per cycle was increased to 15mg with the device always hydraulically connected. A pilot plus main injection strategy was employed; pilot quantity was kept constant at 2mg/str while the main injection quantity was increased to 13mg/str. The average soot emissions are given in Table 6 and Table 7. These results are included in Figure 6. In this test, reduction

410 in soot emissions of 7%, from an average value of 1.84 mg/m³ to average value of 1.71
 411 mg/m³ was observed when the device was powered (WDP conditions). Interestingly the
 412 soot concentration is always lower than tests when the device is not powered (WDNP
 413 conditions) as shown in Figure 6.

414
 415

416 *Table 6 - Test matrix and measurements of torque, BMEP and soot. Total fuel injected 15*
 417 *mg/str. WDNP.*

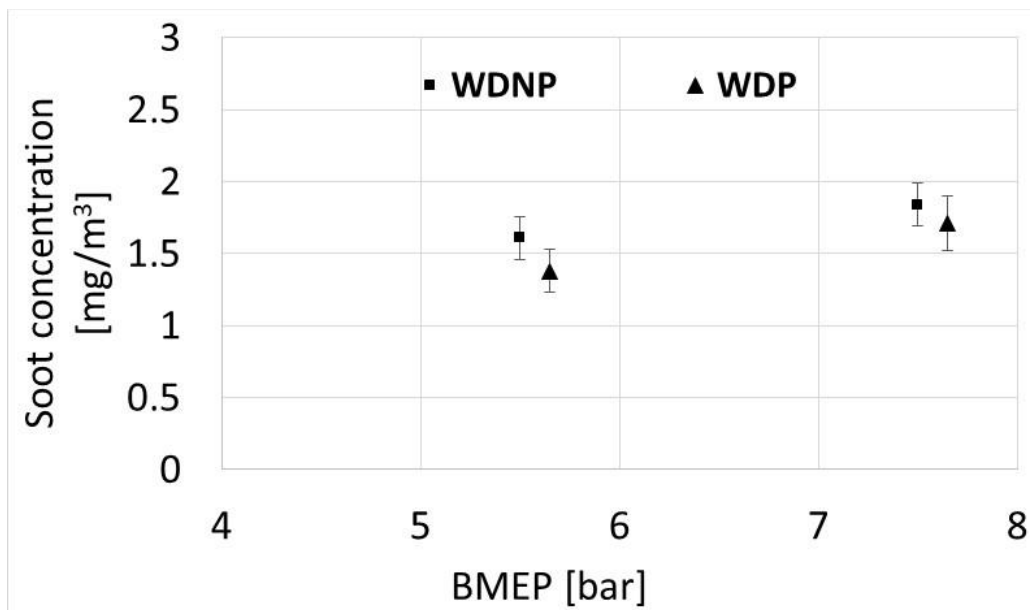
pilot		main		AVG Torque	AVG BMEP	AVG Soot	STD Soot
[°ATDC]	[mg]	[°ATDC]	[mg]	[Nm]	[bar]	[mg/m ³]	[mg/m ³]
-12	2	-4	13	33.7	7.7	1.84	0.15

418
 419

420 *Table 7 - Test matrix and measurements of torque, BMEP and soot. WDP. Total fuel*
 421 *injected 15mg/str.*

pilot		main		AVG Torque	AVG BMEP	AVG Soot	STD Soot
[°ATDC]	[mg]	[°ATDC]	[mg]	[Nm]	[bar]	[mg/m ³]	[mg/m ³]
-12	2	-4	13	33.5	7.6	1.71	0.14

422
 423



425

426 *Figure 6 - Comparison of the average soot concentration collected in WDNP and WDP*
 427 *conditions at two BMEP target values. Injection strategy: pilot plus main injections.*

428

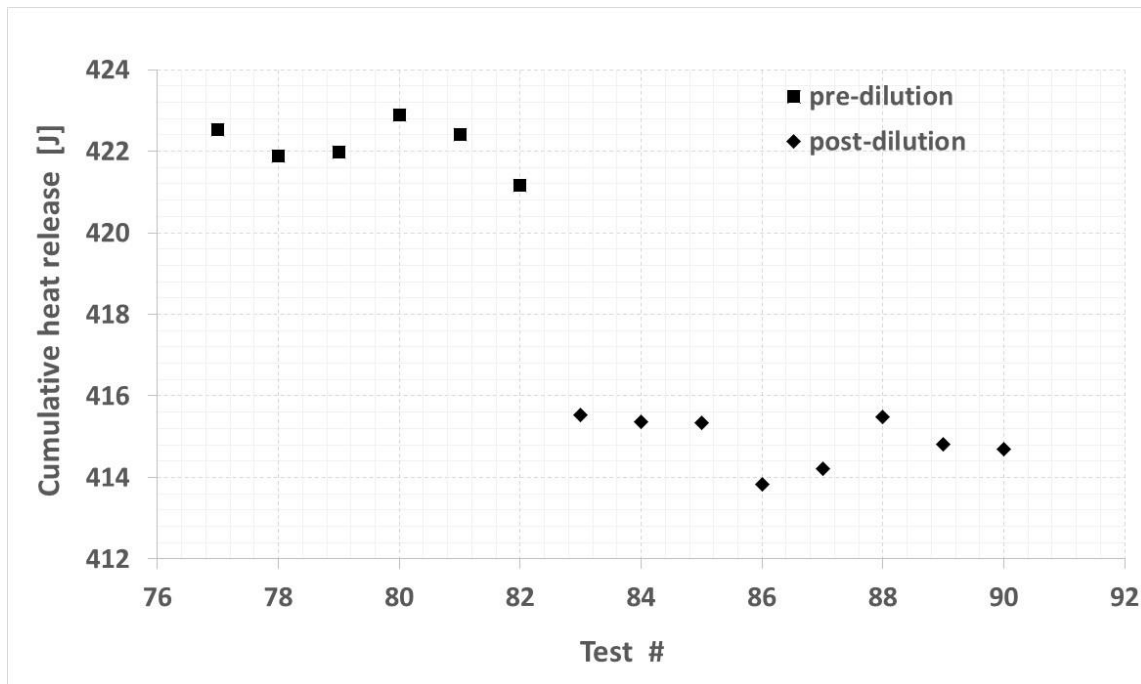
429

430 The hypothesis proposed here to explain the measured reduction in soot emission is linked
 431 to leaching of metals into the fuel. The device is constituted by a 190mm long copper pipe
 432 containing a helicoidally shaped copper duct and therefore a large copper surface area is
 433 in contact with the fuel. Authors had previous experience of copper contamination of the
 434 fuel, when a copper heat exchanger was used during cold start testing, impacting on
 435 engine performance. Fuel contamination due to metal contact has been extensively studied
 436 [22], with presence of copper ions determined by ICP [26]. Metallic additives are well
 437 known in the literature as catalysts for the combustion process and for promoting oxidation
 438 of carbon nanoparticles during combustion [6,11,16,17]. Literature review covering the
 439 state of the art in fuel additives has suggested that additives are typically added to a fuel
 440 in form of nanoparticle powder; these nanoparticles are then dispersed in the base fuel
 441 and remain in suspension. Leaching releases metals in sub-nanometric aggregates or even
 442 ions rather than as nanoparticles so increasing the contact surface area.

443 In the present study, a fuel flow meter installed before the HP fuel pump measured a fuel
444 flow rate of 30kg/h. At the operating condition tested, only 1.44kg/h is delivered to the
445 injector while the remainder is discharged from the pump to return to the fuel tank.
446 Therefore if leaching occurs the fuel borne metallic catalyts are partially recirculated into
447 the fuel tank. This might explain the sharp reduction in soot emission starting from day 2
448 even when the device was not powered (WDNP conditions), as the fuel tank was not refilled
449 during the first day of engine testing. Day 2 started with roughly half a tank of fuel from
450 the previous day, and was refilled towards the middle of the day. On the subsequent days
451 of engine testing the fuel tank was regularly refilled throughout the day. Fuel-borne
452 catalyst concentration build-up can potentially explain the steeper decrease in soot
453 emission in the first two days of testing.

454 Effect of tank top up with fresh fuel was investigated by plotting cumulative heat release
455 calculation of consecutive tests.

456 Figure 7 shows the effect of fuel tank refill on the cumulative heat release. According to
457 our hypothesis, restoring the fuel level in the tank to its maximum, using fresh diesel,
458 dilutes the concentration of metals leached from the device. After a short period of time,
459 a noticeable drop in cumulative heat release was measured. Adding new fuel to the tank
460 seems to have a detrimental impact on the cumulative heat release, as it decreases shortly
461 after tanks is topped up.



462

463 *Figure 7 - Effect of fuel tank top up on cumulative heat release in WDP conditions.*

464

465 A 20ml fuel sample was collected towards the end of the last day of testing. ICP analysis
 466 showed presence of copper in the diesel fuel. Results were compared to the baseline diesel
 467 fuel (0,2ppm Cu); the analysis of the fuel collected directly from the injector of the single
 468 cylinder engine showed an increase in copper concentration from 0.2mg/L to 1mg/L when
 469 the device is connected in the fuel line (see Table 8).

470 However, it was not clear if the metal in the fuel can be associated with wear of the fuel
 471 injection system or rather released by the device. Therefore, a dedicated test rig was used
 472 to assess whether the device is capable to release metals in the fuel. The test rig does not
 473 have other possible sources of metal contamination and is constituted mainly by the device
 474 and a high-density polyethylene (HDPE) tank. ICP analysis of fuel recirculated for 180
 475 minutes shows concentrations of copper in diesel with a cumulative concentration
 476 measured going up to 4.6mg/L with recirculating fuel. Metallic additives in diesel fuel are
 477 effective in reducing particulate emission by enhancing soot nanoparticles oxidation as is
 478 widely reported in the literature.

479

480 *Table 8 - Copper concentration in diesel fuel measured using inductively coupled plasma*
481 *- optical emission spectrometry*

Sample analysed	Concentration [mg/l]	STD [mg/l]
Baseline – Diesel	0.2	0.1
Samples from fuel injector	1	0.1
Diesel fuel recirculated to tank taken after 120minutes	3.7	0.1
Diesel fuel recirculated to tank taken after 180minutes	4.6	0.5

482

483

484 Although the mechanism of leaching is not the focus of this paper, the ICP measurement
485 provided in Table 8 corroborate the hypothesis on the mechanism of soot reduction
486 noticeable from measurements taken in this work, i.e., metal contamination of the fuel act
487 as soot oxidation catalyst. Leaching is a well-known process that involves dissolution of
488 solids into a liquid. It is a natural process but can also be implemented by an industrial
489 process. Albeit the leaching rates of metals can be rather low, the hypothesis proposed
490 here is that the utilisation of the magnetic field generated by the device leads to higher
491 leaching rates of metals into the fuel. This can potentially be an interesting way to add
492 combustion catalysts to a fuel; the additive can be released in sub-nanometric aggregates,
493 even as single atoms or ions, rather than as nanoparticles, and this might enhance its
494 catalytic effectiveness.

495 What is still unclear is the size distribution of the copper nanoparticles in the dispersion
496 and whether this is stable over time. Further work will also need to focus on evaluating
497 the rate of copper deposition into the diesel fuel and its dependence on fuel flow rate and
498 surface temperature.

499

500

501

502

503 **Initiation and early development of combustion**

504

505 Details of the initiation and early development of combustion in a firing engine cylinder
506 are difficult to unravel from cylinder pressure measurements because of the small heat
507 release involved. Commonly, optical techniques are employed which require either engine
508 modifications to provide optical access to the combustion system or, as here, the use of a
509 quiescent optical vessel. Optical studies of the initiation of combustion aided by a glow
510 plug have been reported in several publications [35-38]. These have shown that the site
511 of initiation is in the vicinity of the glow plug surface, and combustion spreads into one or
512 both sprays nearest to the glow plug before the remaining sprays ignite.

513 In complementary studies McGhee [30] and Li et al [33] investigated a range of factors
514 which influence the early stage of diesel spray combustion in a quiescent optical vessel
515 and showed that glow plug temperature and number of pilot injections have the strongest
516 impact on initiation of combustion. The investigations presented in this section were
517 undertaken to clarify the effect of the device on the successful initiation and development
518 of combustion. Of particular interest is its effect on ignition delay and occurrence of a
519 successful initiation.

520 The site of the initial luminous emissions associated with the first high temperature
521 reactions has been identified, with the device powered (WDP) and without the device
522 (WO). A modified version of the test rig used in [33] was employed, including the device
523 installed before the HP pump so that optical analysis of combustion initiation and early
524 development could be carried out. The pilot plus main injection strategies that mimics the
525 engine testing was used. An example of a sequence of images illustrating the successful
526 initiation of combustion is given in Figure 8.

527 Ignition delay is not affected by the presence of the device, but it is more likely to
528 achieve a sustainable combustion when the device is powered.

529

530

531

532

533

	In-cylinder pressure 30bar & glowplug on		In-cylinder pressure 28bar& glowplug on	
	Test 4 Glow plug on (WO conditions)	Test 5 Glow plug on (WDP conditions)	Test 6 Glow plug on (WO conditions)	Test 7 Glow plug on (WDP conditions)
38th frames				
60th frames				
120th frames				
	Device not powered. At an in-cylinder pressure of 30bar combustion initiation occurred. Only one of the fuel plumes close to the glow plug ignites	In-cylinder pressure of 30bar; combustion initiation occurred. When the device is powered the two fuel plumes close to the glow plug ignite	Device not powered. Misfire recorded. When pressure is lowered to 28bar, it was more likely for combustion initiation to fail.	Despite the lower in-cylinder pressure of 28bar, when the device is powered combustion of the fuel did occur.

534 *Figure 8 - Comparison between high speed photography images of combustion initiation*

535 *in a quiescent constant volume optical vessel equipped with HPCR DI fuel injection*

536 *system and a glow plug in WDP and WO conditions.*

537

538 The images in Figure 8 show the initial luminous emissions associated with the first high

539 temperature reactions occurs at the same time (the 38th frame, whether the device is

540 powered or not). Test 4 and test 5 in Figure 8 show that the first spots of luminous

541 emissions appear close to the glow plug tip at the edge of the fuel spray after the start of

542 the main injection. This local initiation triggers a rapid expansion of the enflamed volume,

543 principally in the downstream direction of spray penetration. There were no significant

544 differences in the way a successful initiation was achieved, although subsequent
545 development took place in a different fashion with test 6 showing combustion of both
546 adjacent sprays when the device is powered (test 5). When lowering the chamber pressure
547 to 28 bar (test 6 and 7) initiation failed when the device was not installed (WO). In
548 contrast, when the device was powered initiation was always successful. This ties rather
549 well with the finding from Gumus et al. stating that the use of copper nanoparticles in
550 diesel increases the ignition probability [16].

551

552

553 **Conclusions**

554

555 Soot measurements were taken from a single cylinder DI Diesel engine equipped with a
556 Euro V high pressure common rail fuel injection system and a fuel conditioner device
557 constituted by a helicoidally shaped copper duct embedded within electromagnetic coils.
558 Inductively coupled plasma optical emission spectrometry revealed that copper
559 contamination of the fuel occurred when the device was powered. Fuel collected directly
560 from the injector of the single cylinder engine showed an increase in copper concentration
561 from 0.2mg/L to 1mg/L. A bespoke test rig with fuel recirculating through device showed
562 a copper concentration equal to 4.6mg/l after 180 minutes, significantly higher than the
563 initial concentration, equal to 0.2mg/L; indicating that the device can release copper into
564 the fuel.

565 The engine testing investigation showed that a 7-14% reduction in soot emissions is
566 achieved when the device was connected. The combustion analysis and soot emission
567 measurements suggest that the presence of metals from the helicoidally shaped copper
568 duct into diesel fuel is responsible for the soot reduction and the combustion enhancement
569 measured in this work.

570 High speed photography of combustion initiation in a quiescent constant volume optical
571 vessel equipped with HPCR DI fuel injection system showed that the ignition probability is
572 enhanced when device is used.

573 The catalytic effect of the leached metals in the fuel is thought to be the responsible for
574 the soot reduction mechanism. This is potentially an interesting mechanism for the release
575 of fuel borne catalyst at the point of need. However, further investigation is necessary to
576 quantify the rate of leaching as function of operating conditions, the soot reduction as
577 function of catalyst concentration and the stability of fuel borne catalyst in suspension.

578

579 **Acknowledgements**

580

581 *The authors would like to thank Dukic day dream srl for the supply of the Dukic Day Dream*
582 *(3D) Car devices used in this investigation and for their permission to publish this study.*

583

584 **REFERENCES**

585

- 586 [1] Giechaskiel B, Munoz-Bueno R, Rubino L, Manfredi U, Dilara P, De Santi G, et al.
587 Particle Measurement Programme (PMP): Particle Size and Number Emissions
588 Before, During and After Regeneration Events of a Euro 4 DPF Equipped Light-Duty
589 Diesel Vehicle. JSAE/SAE Int. Fuels Lubr. Meet., SAE International; 2007.
590 doi:<https://doi.org/10.4271/2007-01-1944>.
- 591 [2] Rubino L, Piotr Oles J, La Rocca A. Evaluating Performance of Uncoated GPF in Real
592 World Driving Using Experimental Results and CFD modelling. 13th Int. Conf.
593 Engines Veh., SAE International; 2017. doi:<https://doi.org/10.4271/2017-24-0128>.
- 594 [3] Bonatesta F, Chiappetta E, La Rocca A. Part-load particulate matter from a GDI
595 engine and the connection with combustion characteristics. Appl Energy
596 2014;124:366–76. doi:10.1016/j.apenergy.2014.03.030.
- 597 [4] Yang K, Fox JT, Hunsicker R. Characterizing Diesel Particulate Filter Failure During
598 Commercial Fleet Use due to Pinholes, Melting, Cracking, and Fouling. Emiss Control
599 Sci Technol 2016;2:145–55. doi:10.1007/s40825-016-0036-0.
- 600 [5] Von Stockhausen A, Mangold MP, Eppinger D, Livingston TC. Procedure for
601 Determining the Allowable Particle Contamination for Diesel Fuel Injection

- 602 Equipment (FIE), SAE Int. J. Fuels Lubr. 2(1):294-304, 2009.
603 doi:<https://doi.org/10.4271/2009-01-0870>.
- 604 [6] Kannan GR, Karvembu R, Anand R. Effect of metal based additive on performance
605 emission and combustion characteristics of diesel engine fuelled with biodiesel. Appl
606 Energy 2011;88:3694–703. doi:10.1016/j.apenergy.2011.04.043.
- 607 [7] Shaafi T, Sairam K, Gopinath A, Kumaresan G, Velraj R. Effect of dispersion of
608 various nanoadditives on the performance and emission characteristics of a CI
609 engine fuelled with diesel, biodiesel and blends—A review. Renew Sustain Energy
610 Rev 2015;49:563–73. doi:10.1016/j.rser.2015.04.086.
- 611 [8] Saxena V, Kumar N, Saxena VK. A comprehensive review on combustion and
612 stability aspects of metal nanoparticles and its additive effect on diesel and biodiesel
613 fuelled C.I. engine. Renew Sustain Energy Rev 2017;70:563–88.
614 doi:10.1016/j.rser.2016.11.067.
- 615 [9] Keskin A, Gürü M, Altıparmak D. Influence of metallic based fuel additives on
616 performance and exhaust emissions of diesel engine. Energy Convers Manag
617 2011;52:60–5. doi:10.1016/j.enconman.2010.06.039.
- 618 [10] Lenin MA, Swaminathan MR, Kumaresan G. Performance and emission
619 characteristics of a DI diesel engine with a nanofuel additive. Fuel 2013;109:362–
620 5. doi:10.1016/j.fuel.2013.03.042.
- 621 [11] Mehta RN, Chakraborty M, Parikh PA. Nanofuels: Combustion, engine performance
622 and emissions. Fuel 2014;120:91–7. doi:10.1016/j.fuel.2013.12.008.
- 623 [12] Miller A, Ahlstrand G, Kittelson D, Zachariah M. The fate of metal (Fe) during diesel
624 combustion: Morphology, chemistry, and formation pathways of nanoparticles.
625 Combust Flame 2007;149:129–43. doi:10.1016/j.combustflame.2006.12.005.
- 626 [13] Nash DG, Swanson NB, Preston WT, Yelverton TLB, Roberts WL, Wendt JOL, et al.
627 Environmental implications of iron fuel borne catalysts and their effects on diesel
628 particulate formation and composition. J Aerosol Sci 2013;58:50–61.
629 doi:<https://doi.org/10.1016/j.jaerosci.2013.01.001>.
- 630 [14] Kim K, Hahn DW. Interaction between iron based compound and soot particles in

631 diffusion flame. Energy 2016;116:933–41.
632 doi:<https://doi.org/10.1016/j.energy.2016.09.132>.

633 [15] Keskin A, Gürü M, Altiparmak D. Biodiesel production from tall oil with synthesized
634 Mn and Ni based additives: Effects of the additives on fuel consumption and
635 emissions. Fuel 2007;86:1139–43. doi:10.1016/j.fuel.2006.10.021.

636 [16] Gumus S, Ozcan H, Ozbey M, Topaloglu B. Aluminum oxide and copper oxide
637 nanodiesel fuel properties and usage in a compression ignition engine. Fuel
638 2016;163:80–7. doi:10.1016/j.fuel.2015.09.048.

639 [17] Tyagi H, Phelan PE, Prasher R, Peck R, Lee T, Pacheco JR, et al. Increased hot-plate
640 ignition probability for nanoparticle-laden diesel fuel. Nano Lett 2008;8:1410–6.
641 doi:10.1021/nl080277d.

642 [18] May W, Hirs E. Catalyst for improving the combustion efficiency of petroleum fuels
643 in diesel engines. 11th Diesel Engine Emiss Reduct Conf 2005;1997:1–16.

644 [19] Gan Y, Qiao L. Combustion characteristics of fuel droplets with addition of nano and
645 micron-sized aluminum particles. Combust Flame 2011;158:354–68.
646 doi:10.1016/j.combustflame.2010.09.005.

647 [20] Heeb N V, Ulrich A, Emmenegger L, Czerwinski J, Mayer A, Wyser M. Secondary
648 Emissions Risk Assessment of Diesel Particulate Traps for Heavy Duty Applications.
649 SIAT 2005, The Automotive Research Association of India; 2005.
650 doi:<https://doi.org/10.4271/2005-26-014>.

651 [21] V Heeb N, Zennegg M, Gujer E, Honegger P, Zeyer K, Gfeller U, et al. Secondary
652 Effects of Catalytic Diesel Particulate Filters: Copper-Induced Formation of PCDD/Fs.
653 Environ Sci Technol 2007;41:5789–94. doi:10.1021/es062962x.

654 [22] Norouzi S, Eslami F, Wyszynski ML, Tsolakis A. Corrosion effects of RME in blends
655 with ULSD on aluminium and copper. Fuel Process Technol 2012;104:204–10.
656 doi:<https://doi.org/10.1016/j.fuproc.2012.05.016>.

657 [23] Hu E, Xu Y, Hu X, Pan L, Jiang S. Corrosion behaviors of metals in biodiesel from
658 rapeseed oil and methanol. Renew Energy 2012;37:371–8.
659 doi:<https://doi.org/10.1016/j.renene.2011.07.010>.

- 660 [24] Haseeb ASMA, Masjuki HH, Ann LJ, Fazal MA. Corrosion characteristics of copper
661 and leaded bronze in palm biodiesel. *Fuel Process Technol* 2010;91:329–34.
662 doi:<https://doi.org/10.1016/j.fuproc.2009.11.004>.
- 663 [25] Fazal MA, Haseeb ASMA, Masjuki HH. Degradation of automotive materials in palm
664 biodiesel. *Energy* 2012;40:76–83.
665 doi:<https://doi.org/10.1016/j.energy.2012.02.026>.
- 666 [26] Fazal MA, Haseeb ASMA, Masjuki HH. Comparative corrosive characteristics of
667 petroleum diesel and palm biodiesel for automotive materials. *Fuel Process Technol*
668 2010;91:1308–15. doi:<https://doi.org/10.1016/j.fuproc.2010.04.016>.
- 669 [27] Aquino IP, Hernandez RPB, Chicoma DL, Pinto HPF, Aoki I V. Influence of light,
670 temperature and metallic ions on biodiesel degradation and corrosiveness to copper
671 and brass. *Fuel* 2012;102:795–807.
672 doi:<https://doi.org/10.1016/j.fuel.2012.06.011>.
- 673 [28] Barth EA. EPA evaluation of the Gastell device under section 511 of the Motor Vehicle
674 Information and Cost Savings Act. Technical report 1981.
- 675 [29] Penninga ,. EPA (Environmental Protection Agency) evaluation of Fuel Maximiser TM
676 under Section 511 of The Motor Vehicle Information And Cost Savings Act. Technical
677 report 1981.
- 678 [30] McGhee M, Shayler PJ, LaRocca A, Murphy M, Pegg I. The Influence of Injection
679 Strategy and Glow Plug Temperature on Cycle by Cycle Stability Under Cold Idling
680 Conditions for a Low Compression Ratio, HPCR Diesel Engine *SAE Int. J.*
681 *Engines* 5(3):923-937, 2012, doi:<https://doi.org/10.4271/2012-01-1071>.
- 682 [31] McGhee, M. et al. Investigations of injection strategies for stable cold idling of an
683 HPCR diesel engine with a compression ratio of 15.5: 1, in *Fuel Systems for IC*
684 *Engines*. Elsevier 2012:167–82.
- 685 [32] MacMillan DJ, Rocca A La, Shayler PJ, Murphy M, Pegg I, Morris T. Comparison of
686 the indicated work outputs, idle stabilities, and heat release characteristics of a
687 direct-injection diesel engine operating cold at two compression ratios. *Proc Inst*
688 *Mech Eng Part D J Automob Eng* 2010;224:799–813.

689 doi:10.1243/09544070JAUTO1328.

690 [33] Li Q, Shayler PJ, McGhee M, Rocca A La. The initiation and development of
691 combustion under cold idling conditions using a glow plug in diesel engines. *Int J*
692 *Engine Res* 2017;18:240–55. doi:10.1177/1468087416652266.

693 [34] Heywood JB. *Internal Combustion Engine Fundamentals*. McGraw-Hill; 1988.

694 [35] Pacaud P, Perrin H, Laget O. Cold Start on Diesel Engine: Is Low Compression Ratio
695 Compatible with Cold Start Requirements? *SAE Int. J. Engines* 1(1):831-849, 2009
696 doi:<https://doi.org/10.4271/2008-01-1310>.

697 [36] Walter B, Perrin H, Dumas JP, Laget O. Cold Operation with Optical and Numerical
698 Investigations on a Low Compression Ratio Diesel Engine, *SAE 2009 Powertrains*
699 *Fuels and Lubricants Meeting*, pp 186-204 vol.2 iss.2.
700 doi:<https://doi.org/10.4271/2009-01-2714>.

701 [37] Chartier C, Aronsson U, Andersson Ö, Egnell R. Effect of Injection Strategy on Cold
702 Start Performance in an Optical Light-Duty DI Diesel Engine. *SAE Int J Engines*
703 2009;2:431–42. doi:10.4271/2009-24-0045.

704 [38] Mueller CJ, Musculus MP. Glow Plug Assisted Ignition and Combustion of Methanol
705 in an Optical DI Diesel Engine. *Int. Spring Fuels Lubr. Meet.*, SAE International;
706 2001. doi:<https://doi.org/10.4271/2001-01-2004>.

707

708